Sundaralingam, M. (1972) *Ann. N.Y. Acad. Sci. 195*, 324–355.
Tamm, L. K., & Seelig, J. (1983) *Biochemistry 22*, 1474–1483.
Watts, A., Harlos, K., & Marsh, D. (1981) *Biochim. Biophys. Acta 654*, 91–96.
Wohlgemuth, R., Waespe-Sarcevic, N., & Seelig, J. (1980) *Biochemistry 19*, 3315–3321.

Structural Determination of Oligosaccharides Derived from Lipooligosaccharide of *Neisseria gonorrhoeae* F62 by Chemical, Enzymatic, and Two-Dimensional NMR Methods†

Ryohei Yamasaki,*,‡,§ Bradley E. Bacon,§ Wade Nasholds,‡,§ Herman Schneider,∥ and J. M. Griffiss‡,§

Center for Immunochemistry and Department of Laboratory Medicine, University of California, San Francisco, and Veterans Administration Medical Center (113A), San Francisco, California 94121, and Walter Reed Research Institute, Washington, D.C. 20307

Received May 10, 1991; Revised Manuscript Received July 30, 1991

ABSTRACT: F62 LOS of *Neisseria gonorrhoeae* consists of two major LOS components; the higher and smaller molecular weight (MW) components were recognized by MAbs 1-1-M and 3F11 respectively. Base-line separation of the two major oligosaccharide (OS) components from F62 LOS was achieved by Bio-Gel P-4 chromatography after dephosphorylation of the OS mixture. The structures of the two major OSs were studied by chemical, enzymatic, and 2D NMR methods [double quantum filtered COSY (DQF-COSY), delayed COSY (D-COSY), homonuclear Hartmann–Hahn spectroscopy (HOHAHA), pure-absorption 2D NOE NMR] as well as methylation followed by GC/MS analysis. The OS component derived from the MAb 1-1-M defined LOS component was determined to have a V^3-(β-*N*-acetylgalactosaminyl)neolactotetraose structure (GalNAc is β1→3-linked to a neolactotetraose) at one of its nonreducing termini as shown below. The above pentaose is linked to a branched diheptose–KDO core in which a GlcNAc is α-linked. The OS component derived from the MAb 3F11 defined LOS component did not have a GalNAc residue. The rest of its structure was identical to that of the OS-1, and a neolactotetraose is exposed at its nonreducing terminus.

GalNAcβ1→3Galβ1→4GlcNAcβ1→3Galβ1→4Glcβ1→4Hepα→KDO
3
↑
GlcNAcα1→2Hepα1

Lipooligosaccharides (LOSs)[1] are important antigenic and pathogenic components of the outer membrane of *Neisseria gonorrhoeae*. Gonococcal LOSs cause severe damage to fallopian tubes (Gregg et al., 1981) and are also target molecules for bactericidal activity by normal human sera (Schoolnik et al., 1976). The heterogeneity of gonococcal LOSs in relation to their antigenicities has been extensively investigated. Schneider et al. (1984) showed that gonococcal LOSs consist of several components with molecular weights ranging from 3200 to 7100. Immunochemical analysis of gonococcal LOSs using several murine monoclonal antibodies (MAbs) has shown that gonococcal LOSs consist of discrete individual LOS components, which indicates that the antigenic heterogeneity is due to structural heterogeneity of LOS components (Schneider et al., 1984; Mandrell et al., 1986). Out of several murine MAbs studied, 1-1-M, 3F11, and O6B4 (all IgM) were found to bind to almost all gonococcal LOSs.

Recent immunochemical characterization of human blood group antigen precursors by MAbs 3F11 and O6B4 revealed that the antigenic similarity exists between gonococcal LOSs and glycosphingolipids (Mandrell et al., 1988). Mandrell et al. showed that the two MAbs bind to neutral glycosphingolipids carrying *N*-acetyllactosamine (Galβ1→4GlcNAc) at their nonreducing termini. Further, Stromberg et al. (1988) identified a gonococcal surface component, distinct from pilin and protein II, that binds to epithelial surface glycolipids. This surface component was further investigated and suggested to

† This work was supported by NIH grants (AI 22998 and AI 22160). This is Report No. 44 from the Center for Immunochemistry, University of California, San Francisco.

* Address correspondence to this author at UCSF/VAMC 113A, 4150 Clement St., San Francisco, CA 94121.
‡ University of California.
§ VA Medical Center.
∥ Walter Reed Research Institute.

[1] Abbreviations: 2D, two dimensional; COSY, two-dimensional correlation spectroscopy; DQF-COSY, double quantum filtered COSY; D-COSY, delayed COSY; Gal, galactose; GalNAc, *N*-acetylgalactosamine; Glc, glucose; GC, gas chromatography; GlcNAc, *N*-acetylglucosamine; Hep, heptose; HF, hydrofluoric acid; HOHAHA, homonuclear Hartmann–Hahn spectroscopy; KDO, 2-keto-3-deoxy-mannooctulosonic acid; LOS, lipooligosaccharide; MAb, monoclonal antibody; MS, mass spectrometry; NMR, nuclear magnetic resonance; NOE, nuclear Overhauser effect; OS, oligosaccharide; TFA, trifluoroacetic acid.

0006-2960/91/0430-10566$02.50/0

be a protein of MW 36 000 (Paruchuri et al., 1990). Their findings and the antigenic similarity between the gonococcal LOS and the glycosphingolipids suggest that gonococcal adhesion to the cell surface is a complicated process where the LOS play some role. Thus, structural characterization of the LOS is very important to understand the antigenicity and immunogenicity of the gonococcus.

We studied the expression of gonococcal LOS epitopes using a LOS from a serum-sensitive strain F62 as a model with murine IgM MAbs 1-1-M and 3F11 (Yamasaki et al., 1988, 1991). F62 LOS of *N. gonorrhoeae* consists of two components. The higher molecular weight (MW) component is recognized by monoclonal antibody (MAb) 1-1-M and the smaller MW component with MAbs 3F11 and O6B4. The F62 LOS was chemically modified in various ways, and epitope expression of the chemically modified LOS samples revealed the following: (1) The IgM MAb defined epitopes exist in the carbohydrate moiety of the LOS. However, the oligosaccharide (OS) moiety must be in certain conformations which are preserved by the lipoidal moiety. Because of this reason, OS components alone are not recognized by the MAbs. (2) Expression of the MAb-defined epitopes is conformational, and their conformations are governed by the overall structures of LOS. This secondary LOS structure is stabilized by the lipoidal moiety, and the loss of some fatty acids leads to the disorganization of LOS, resulting in the loss of antigenicity. (3) Phosphates and carboxyl groups in the LOS molecule are not involved in the IgM MAb defined epitopes.

We further investigated epitope expression of the two F62 LOS components and their partial structures. F62 LOS was treated with several glycosidases, and expression of epitopes of enzyme-treated LOS samples was analyzed with the two mouse IgM MAbs (Yamasaki et al., 1991). The 1-1-M-defined LOS component was cleaved with both β-*N*-acetylhexosaminidase and endo-β-galactosidase, and each cleavage resulted in the loss of expression of the MAb 1-1-M defined epitope. The *N*-acetylhexosamine (HexNAc) released by the hexosaminidase was determined to be GalNAc, and the smaller oligosaccharide released by the endo enzyme was identified to be a dimer GalNAcβ→Gal. In contrast, the MAb 3F11 defined LOS component was not digested by the endogalactosidase, but it was cleaved with β-galactosidase, which resulted in the loss of its antigenicity. However, MAb 3F11 bound to the MAb 1-1-M defined LOS component after the removal of GalNAc. This characterization of the MAb 1-1-M and 3F11 defined epitopes by glycosidases indicated the following: (1) MAbs 1-1-M and 3F11 both recognize the nonreducing termini of the LOS components; (2) the 1-1-M-defined LOS component has the GalNAcβ→Galβ1→4Glc (or GlcNAc) structure, and the GalNAcβ→Gal moiety is involved in the MAb 1-1-M defined epitope; (3) the MAb 3F11 defined LOS component has a β-Gal residue at its nonreducing terminus, and this residue is involved in the MAb 3F11 defined epitope; (4) the two LOS components share a similar antigenic structure, and the 3F11-defined epitope structure is present in the MAb 1-1-M defined LOS component. Expression of this epitope within the 1-1-M-defined LOS molecule is blocked by the β-GalNAc residue.

In order to define epitope expression of the F62 LOS components, we determined the structures of the two OS components derived from the MAb 1-1-M and 3F11 defined LOS components by chemical, enzymatic, and two-dimensional (2D) NMR (DQF-COSY, HOHAHA, and NOE) methods. Prior to the analysis, we accomplished base-line separation of the dephosphorylated F62 OS components. Each OS component and its enzyme-treated OS components were analyzed extensively by chemical, enzymatic, and 2D NMR methods. The OS components, OS-1 and OS-2, obtained from the MAb 1-1-M and 3F11 defined LOS components were found to be a nonaose and an octaose, respectively, and they both have the same branched diheptose structure. The MAb 1-1-M defined OS component has a V^3(β-*N*-acetylgalactosaminyl)neolactotetraose in which GalNAc is β1→3-linked to a neolactotetraose at one of the nonreducing termini. This pentaose is β-linked to a branched diheptose–KDO core, in which GlcNAc is α-linked to one of the heptoses. The MAb 3F11 defined OS does not have a terminal GalNAc, and a neolactotetraose is exposed at its nonreducing terminus. The structural difference of the two OS components is GalNAc.

Materials and Methods

The F62 LOS of *N. gonorrhoeae* has been characterized previously (Schneider et al., 1982; Yamasaki et al., 1988, 1991). The F62 OS was prepared after the hydrolysis (1% AcOH, 2 h at 100 °C) (Yamasaki et al., 1988). Dephosphorylation of the OS mixture was conducted by treating the OS with aqueous HF (48%) [the intact OS/HF, 10–20 μg/μL] for 24–48 h at 4 °C. After the removal of HF in vacuo, the resulting OS samples were passed through a Bio-Gel P-2 column (1.6 × 80 cm, water as eluate). Fractions containing OS (V_0) were pooled, lyophilized, and then examined by ^{31}P NMR. The HF-treated OS components were analyzed by ascending chromatography over a Bio-Gel P-4 column (<400 mesh, 1.6 × 70 cm). Chromatographic separation of the dephosphorylated OS components in a preparative scale was conducted using a Bio-Gel P-4 column (<400 mesh, 2.6 × 90 cm, 100 mM ammonium acetate) or the two P-4 columns (2.6 × 180 cm) that were connected in tandem. Desalting of OS samples was performed by chromatography on a Bio-Gel P-2 column (<400 mesh, 2.6 × 90 cm).

Enzymatic treatments of OS samples were performed at 37 °C for 16–24 h, and the enzymes were inactivated by heating the mixtures for 3 min at 100 °C. Endo-β-galactosidase was kindly provided by Dr. Michiko Fukuda (La Jolla Cancer Research Foundations, La Jolla, CA). β-*N*-Acetylhexosaminidase (from jack beans) and β-galactosidase (from *Aspergillus niger*) (both from Sigma Chemical Co., St. Louis, MO) were predialyzed in 50 mM sodium acetate buffer (pH 4.5) as described previously (Yamasaki et al., 1991). The OS-1 (800 μg) was treated with 0.08 unit of endo-β-galactosidase in 200 mM sodium acetate (pH 4.5), and it (100 μg) was also treated with 1 unit of β-*N*-acetylhexosaminidase. The OS-2 (680 μg) was treated with 24 units of β-galactosidase. Each enzyme solution was passed through a C18 cartridge (Millipore, Milford, MA), and the resulting solution was applied to a Bio-Gel P-2 column (2.6 × 90 cm) that was equilibrated in water. Each V_0 fraction was collected and then lyophilized.

Compositional analysis of the F62 OS components was performed by hydrolyzing the OS components under the following acidic conditions: 0.25 M H_2SO_4 and 1–4 M TFA for 2–4 h at 100 °C. The monosaccharides released were analyzed by high-performance anion-exchange chromatography (Hardy et al., 1988) or by GC analysis after the alditol acetate derivatization. KDO was analyzed as previously reported (Osborn, 1983; Yamasaki et al., 1988). OS samples were methylated by treating them with NaOH in DMSO (Ciucanu & Kerek, 1984) and then by treating the mixtures with methyl iodide. The partially methylated OS samples were hydrolyzed, reduced with $NaBD_4$, and acetylated (Levery & Hakomori, 1987). The alditol acetate derivatives of partially

methylated carbohydrates were analyzed by gas chromatography (GC) and gas chromatography/mass spectrometry (GC/MS). GC was performed by using a Perkin-Elmer 8500 gas chromatograph equipped with a flame-ionization detector (helium as a carrier gas). GC/MS was performed by interfacing the 8500 gas chromatograph with a Perkin-Elmer ion trap detector. EI mass spectra were recorded at 80 eV. A fused silica column SP2330 (0.25 mm × 30 m, Supelco, Bellefonte, PA) was used for the analysis of alditol acetates (the temperature program for the splitless mode: T_1 = 32 °C for 4 min; 8 °C/min; T_2 = 200 °C for 20 min). The DB1 column (0.25 mm × 30 m, J & W, Folsom, CA) was used for the analysis of partially methylated alditol acetates (the temperature program for the splitless mode: T_1 = 32 °C for 4 min; 8 °C/min; T_2 = 120 °C; 4 °C/min; T_3 = 280 °C for 10 min). Alditol acetate derivatives of partially methylated hexoses and hexosamines were purchased from Biocarbo Chemicals (Lund, Sweden). The relative retention times of some of the above alditol acetate derivatives were as follows: 2,3,4,6-tetra-*O*-methylgalactose, 0.93; 2,3,6-tri-*O*-methylgalactose, 1.00; 2,3,6-tri-*O*-methylglucose, 1.01; 2,4,6-tri-*O*-methylglucose and 2,4,6-tri-*O*-methylgalactose, 1.02; 2-acetamido-2-deoxy-*N*-methyl-3,4,6-tri-*O*-methylglucose, 1.18; 2-acetamido-2-deoxy-*N*-3,4,6-tri-*O*-methylgalactose, 1.22; 2-acetamido-2-deoxy-*N*-methyl-3,6-di-*O*-methylglucose, 1.25. Authentic samples of D- and L-*glycero*-D-*manno*-heptoses and the EI mass spectra of alditol acetates of partially methylated heptoses (3-*O*-methyl and 3,7-di-*O*-methyl) were kindly provided by Dr. O. Horst (Institute for Experimental Biology and Medicine, Borstel, FRG). The nomenclature to describe parts of gonococcal oligosaccharides such as a neolactotetraose and a V^3-(β-*N*-acetylgalactosaminyl)neolactotetraose is according to a review article by Stults et al. (1989).

The high-performance anion-exchange chromatography system (Dionex, Sunnyvale, CA) consisted of a Quaternary gradient pump, a pulsed amperometric detector with gold electrode, a liquid chromatographic module (LCM-2), and a Basic Post column delivery system. A CarboPac PA 1 column (4.6 × 250 mm) and a CarboPac PA guard column (3 × 25 mm) (Dionex, Sunnyvale, CA) were used for the carbohydrate analysis (flow rate 1.0 mL/min; amperometric detection 30–1000 nA). Hexoses and hexosamines were eluted with 10 mM NaOH. Under the conditions used, the typical retention times of galactosamine, glucosamine, galactose (Gal), and glucose (Glc) were 13.4, 16.5, 18.0, and 19.9 min, respectively. Heptoses were eluted with 70 mM NaOH, and the typical retention times for D-*glycero*-D-*gluco*-heptose, L-*glycero*-D-*manno*-heptose, D-*glycero*-D-*manno*-heptose were 15.4, 9.9, 17.8 min, respectively.

^{1}H chemical shifts are relative to the chemical shift of HOD which was calibrated relative to 3,3,3-trimethyl[2,2,3,3-$^2H_4$]propionate (TSP) as a function of temperature. ^{1}H (500-MHz) and ^{31}P (202-MHz) NMR experiments were performed on a GE NMR spectrometer (5-mm probe) at 19.8 °C unless otherwise stated. The OS samples (500–1000 μg) were repeatedly lyophilized in D_2O and were finally dissolved in D_2O (0.4 mL). The spectral width for 2D NMR experiments of OS samples was ±1602 Hz unless otherwise stated.

The double quantum filtered COSY (DQF-COSY) spectra of the dephosphorylated OS-1, endo-OS-1, OS-2, and β-galactosidase-treated OS-2 (Neuhaus et al., 1985; Rance et al., 1983) were acquired in the phase-sensitive mode using time-proportional phase incrementation (TPPI) (Redfield & Kunz 1975). The 0.5K × 4K data points were processed with shifted sine bell functions in the t_1 and t_2 dimensions, respectively, and

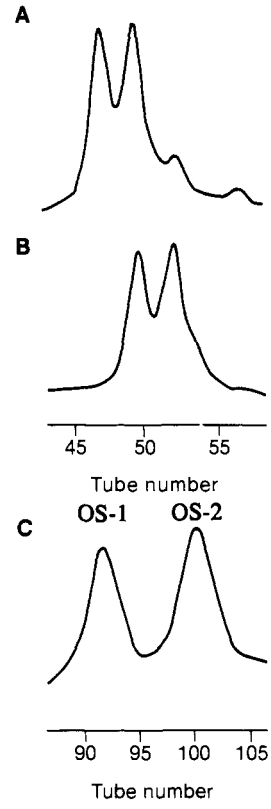

FIGURE 1: Partial chromatograms of the intact and dephosphorylated F62 OS mixtures. Ascending chromatography was conducted using a Bio-Gel P-4 (<400 mesh) in 100 mM ammonium acetate and monitored by a refractometer: (A) P-4 chromatogram of the intact F62 mixture (column: 2.6 × 90 cm, 4.5 mL/tube, V_0 and V_t volumes ~175 and ~410 mL, respectively); (B) P-4 chromatogram of the dephosphorylated F62 OS mixture (chromatographic conditions were same as in panel A); (C) P-4 chromatogram of the dephosphorylated F62 OS mixture (column: 2.6 × 180 cm, 4.1 mL/tube, V_0 and V_t volumes ~340 and ~800 mL, respectively).

were zero-filled to give 1K × 4K real data points. The delayed acquisition COSY (D-COSY) of the dephosphorylated OS-1 and endo-OS-1 were conducted with a 100-ms delay. The 0.5K × 2K data were zero-filled to give 1K × 4K real data points.

Homonuclear Hartmann–Hahn (HOHAHA) (Bax et al., 1985; Yamasaki, 1988) spectra of the dephosphorylated OS-1 (τ_m = 150 ms), endo-OS-1 (τ_m = 50, 70, and 150 ms), and OS-2 (τ_m = 150 ms) were obtained as 0.5K × 4K data points. Fourier transformations were performed with zero filing in the t_1 dimension to give 1K × 2K real data points. The number of acquisitions n was 32, and FIDs were apodized in the t_1 and t_2 dimensions by shifted sine bell functions for resolution enhancement.

Pure-absorption 2D NOE spectra of the dephosphorylated OS-1 (τ_m = 30 and 200 ms) and endo-OS-1 (τ_m = 200 ms) were obtained as 0.5K × 4K data points (States et al., 1982; Yamasaki & Bacon, 1991). The preparation delay time was 5 s. The number of acquisitions n was 32, and the carrier frequency was set at the HOD resonance (4.84 ppm). The data matrix was apodized in both dimensions by shifted sine bell functions for resolution enhancement and zero-filled to give 1K × 2K real data points.

Results and Discussion

The F62 OS mixture was obtained after the hydrolysis of F62 LOS with 1% acetic acid (2 h at 100 °C) and first fractionated by a Bio-Gel P-4 (2.6 × 90 cm) (Yamasaki et al., 1988), and two major components (OS-1 and OS-2) as

shown in Figure 1A. Although partial separation of each of OS component was achieved, the NMR spectra and the carbohydrate compositions of fractions containing each OS component were almost identical, which indicated that each OS preparation is still a mixture of two components. Separation of the two intact OS components was not achieved even by chromatography of the F62 OS mixture with a 200 × 2.6 cm column of P-4 (data not shown). In addition, ^{31}P NMR analysis of the two OS components indicated the presence of phosphorus. This heterogeneity also made it difficult to analyze NMR data as will described below.

To avoid the complexities arising from incomplete separation of OS components, the OS components were dephosphorylated with aqueous HF (48%) at 4 °C. The HF-treated OS components were analyzed by ^{31}P NMR and chromatography to determine the effective level of dephosphorylation as well as to determine the stabilities of the OS. For ^{31}P NMR analysis, the HF-treated OS components were passed through a P-2 column (1.6 × 80 cm, water) and then examined. For chromatographic analysis, we used a P-4 column (1.6 × 70 cm, 100 mM ammonium acetate) that resolved the dephosphorylated OS components (up to 250 μg of each OS). We found that HF treatment [10–20 μg/μL (intact OS/HF), 24 h at 4 °C] is effective to dephosphorylate the intact OS without causing degradations of the OS components. In order to prepare each dephosphorylated OS component in a preparative scale, the dephosphorylated OS mixture was chromatographed on a 2.6 × 90 cm column of Bio-Gel P-4 (Figure 1B), but each dephosphorylated OS component was not resolved well. However, their base-line separation was achieved by using two P-4 columns connected in tandem (Figure 1C). We obtained ~1 mg of each dephosphorylated OS by the above tandem chromatography of the dephosphorylated F62 OS mixture (10 mg) followed by desalting each OS component.

The identity of each OS component was established as previously described: the larger and smaller MW OSs are the MAb 1-1-M and 3F11 defined OS components, respectively (Yamasaki et al., 1991). Compositional analysis of the dephosphorylated OS components was originally carried out by hydrolysis of OS in 1 M trifluoroacetic acid (TFA) (2 h at 100 °C) or 0.25 M sulfuric acid (15 h at 100 °C) and followed by GC analysis after alditol derivatization. Although we confirmed the presence of the carbohydrate components reported in an earlier work (Schneider et al., 1982), the above hydrolysis conditions were found to be inadequate even for the release of hexoses from the OS. We performed series of hydrolysis of OS in 2 or 4 M TFA and analyzed the hydrolyzates by high-performance anion-exchange chromatography with amperometric detection (Hardy et al., 1988). For the release of hexoses and hexosamines from each OS component, hydrolysis with higher concentrations of TFA was necessary (4 M TFA, 2–3 h at 100 °C). The carbohydrate composition of OS-1 was found to be as follows: glucose (Glc):galactose (Gal):heptose (Hep):*N*-acetylglucosamine (GlcNAc):*N*-acetylgalactosamine (GalNAc):*manno*-octulosonic acid (KDO), 1:2:2:2:1:1. The carbohydrate composition found in the OS-2 is the same as in the OS-1 except for the absence of GalNAc. The identity of the Hep present in OS-1 and OS-2 was found to be L-*glycero*-D-*manno*-heptose by high-performance anion-exchange chromatography. The manno configuration was also confirmed by NMR analysis as will be described later.

Figure 2A shows the ^1H NMR spectrum of the intact OS-1, and some peaks present in the higher anomeric region were found to be due to the protons that are coupled to ^{31}P. This is clear from Figure 2B, which is a part of the difference spectrum that was obtained by subtracting the ^{31}P-decoupled ^1H NMR spectrum of the intact OS-1 from Figure 2A. The inverted peaks in Figure 2B show the protons involved in the ^{31}P–^1H coupling. The ^1H NMR spectrum of the dephosphorylated OS-1 is shown in Figure 2C. The spectrum of the dephosphorylated OS-1 showed the resonances of its anomeric protons between 5.60 and 4.40 ppm, the CH_3 resonances (at 2.05 ppm) of *N*-acetylhexosamine residues, and the resonances of the deoxy (methylene) protons (at 1.185, 1.325, 1.915, and 2.410 ppm) presumably due to the KDO residue at the reducing end, as well as the remaining resonances between 4.30 and 3.40 ppm. Although a few protons were shielded in the lower field after dephosphorylation and two sets of two protons almost overlapped, we could identify three α and four β anomeric protons as found in the intact OS-1. From the 1D NMR and compositional analysis, the OS-1 and OS-2 were found to be a nonaose and an octaose, respectively. We confirmed that there were no protons hidden within the HOD peak by examining the NMR spectra of the dephosphorylated OS-1 and OS-2 at 59.8 °C (data not shown).

In order to facilitate the NMR analysis, the dephosphorylated OS-1 was cleaved by exo-β-*N*-acetylhexosaminidase and endo-β-galactosidase (Yamasaki et al., 1991). As reported previously, the β-hexosaminidase cleaves the terminal β-*N*-acetylgalactosaminyl residue of the OS-1, and the endo enzyme cleaves the internal β-galactosidic linkage of the OS-1 into a disaccharide, GalNAcβ→Gal, and an oligosaccharide which was found to be a heptaose in the present study. This heptaose is shown as an example in Figure 2D. By comparative analysis of 1D spectra of the dephosphorylated OS-1 and its enzyme-treated OS-1 samples, the anomeric protons at 4.617 and 4.480 ppm of the dephosphorylated OS-1 were found to be due to GalNAc (V) and Gal (VII), respectively. The dephosphorylated OS-2 gave the identical spectrum to Figure 2D after the β-galactosidase treatment, and the spectrum of the β-hexosaminidase-treated OS-1 was almost identical to that of the dephosphorylated OS-2 (data not shown). These results suggested that the OS-1 is a β-*N*-acetylgalactosaminilated OS-2.

Dephosphorylated OS samples (OS-1, OS-2, and their enzyme-treated OS) were extensively analyzed by 2D NMR spectroscopy: double quantum filtered COSY (DQF-COSY), delayed COSY (D-COSY), homonuclear Hartmann-Hahn spectroscopy (HOHAHA), and pure-absorption 2D NOE NMR as well as methylation followed by GC/MS analysis. We assigned ring and exocyclic protons of each carbohydrate residue and determined vicinal coupling constants by comparatively analyzing DQF-COSY, D-COSY (data not shown), HOHAHA, and NOE spectral data of the dephosphorylated OS-1, OS-2, and its enzyme-cleaved products. The chemical shifts and coupling constants of the dephosphorylated OS-1, endo-OS-1 (the heptaose), and OS-2 are presented in Table I.

Since the carbohydrate compositions of the dephosphorylated OS components are known (Schneider et al., 1982; Yamasaki et al., 1991), the rest of anomeric protons (5.566, 5.095, 5.075, 4.720, 4.555, and 4.470 ppm) were identified from the coupling constants of the ring protons that were obtained from the comparative spectral (D-COSY, DQF-COSY, and HOHAHA) analysis. The gluco and galacto configurations were distinguished from their $J_{3,4}$ and $J_{4,5}$: the $J_{3,4}$ and $J_{4,5}$ of the former are both large (~9 Hz), and the $J_{3,4}$ and $J_{4,5}$ of the latter are large and small (~4 Hz), respectively. The DQF-COSY spectra of the dephosphorylated

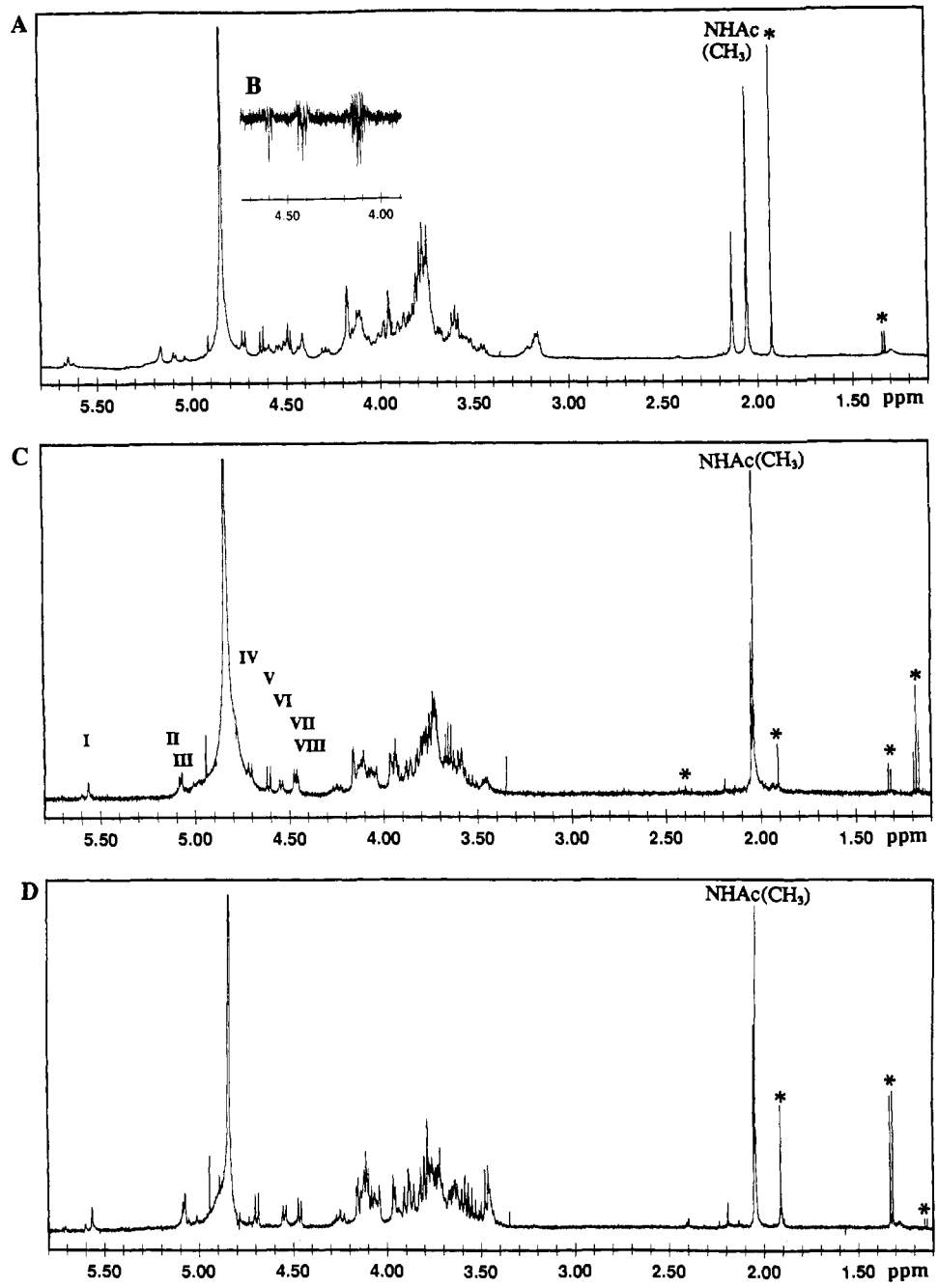

FIGURE 2: ^{1}H NMR spectra of the intact and dephosphorylated OS-1 at 19.8 °C: (A) intact OS-1; (B) spectrum obtained by subtracting the ^{31}P-decoupled spectrum from that in panel A; (C) dephosphorylated OS-1; (D) endo-OS-1, the hepatose obtained from the dephosphorylated OS-1 after the endo enzyme treatment. I, ManHep; II, GlcNAc; III, ManHep; IV, GlcNAc; V, GalNAc; VI, Glc; VII, Gal; VIII, Gal. (*) KDO deoxy protons.

OS-1 and endo-OS-1 are shown in Figures 3 and 4, respectively.

As shown in Figure 5, the HOHAHA spectrum (τ_m = 150 ms) contained almost all of scalar connectivities of the three anomeric protons at 5.095 (II), 4.720 (IV), and 4.555 (VI) ppm. From their $J_{2,3}$, $J_{3,4}$, and $J_{4,5}$ values (Table I), II, IV, and VI were identified to have the gluco configuration. Since the molar ratio of Glc and GlcNAc is 1:2, one of the three anomeric protons is Glc, and as will be described later, VI was found to be Glc. Similarly, the β-anomeric proton (VIII) was identified to be due to Gal. From the large $J_{4,5}$ and the small $J_{2,3}$ and $J_{3,4}$ coupling constants (Table I), the two α-anomeric protons, I and III, at 5.566 and 5.078 ppm were determined to be due to the carbohydrates having manno configurations, and they were identified as L-*glycero*-D-*manno*-heptose, the presence of which was confirmed as already described.

The oligosaccharide sequence was determined by pure-absorption 2D NOE NMR and methylation analysis (Table II). Figure 6 shows the typical NOE spectrum of the dephosphorylated OS-1 of τ_m = 200 ms, and almost all of the intra- and interresidual NOEs in the figure were also detected in the 2D NOE spectrum of τ_m = 35 ms when plotted at the same contour level (data not shown). Further, the NOE spectrum of the endo-OS-1 (τ_m = 200 ms) (data not shown) was almost identical to that of its parent OS except for the absence of intra- and interresidual NOEs due to a disaccharide residue, GalNAc(V)–Gal(VII).

As expected from the distances (~2.6 Å) between the 1,3-diaxially oriented protons in the $^4C_1$ conformation, the intraresidual NOEs due to the H1–H3 and H1–H5 were detected with the β-linked residues such as IV (GlcNAc), V (GalNAc), and VI (Glc) (Figure 6). The assignment of H-5

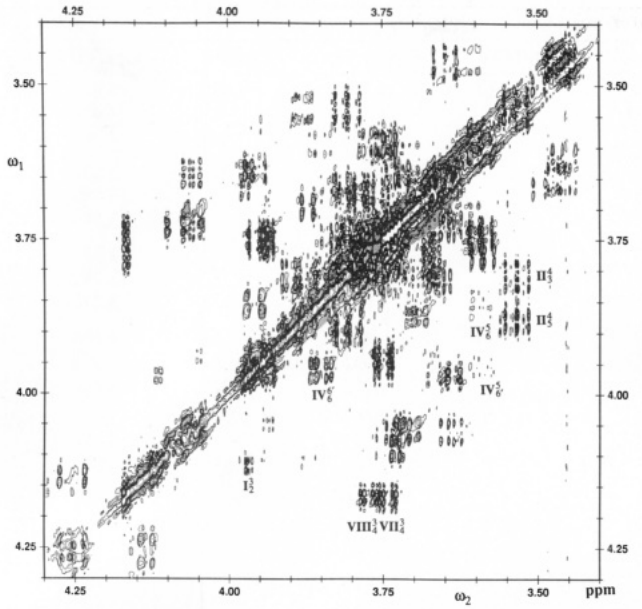

FIGURE 3: DQF-COSY spectrum (4.30–3.40 ppm) of the dephosphorylated OS-1 at 19.8 °C. Negative levels are shaded. The digital resolution of the spectrum is 0.78 Hz. Only some of the cross-peaks are labeled. Roman numerals refer to the carbohydrate residue (see Figure 2C and Table I), and Arabic numerals refer to the protons in the respective sugar residues. The superscript refers to the proton whose chemical shift is given on the ω_2 axis, and the subscript refers to the proton whose chemical shift is given on the ω_1 axis. I, ManHep; II, GlcNAc; III, ManHep; IV, GlcNAc; V, GalNAc; VI, Glc; VII, Gal; VIII, Gal.

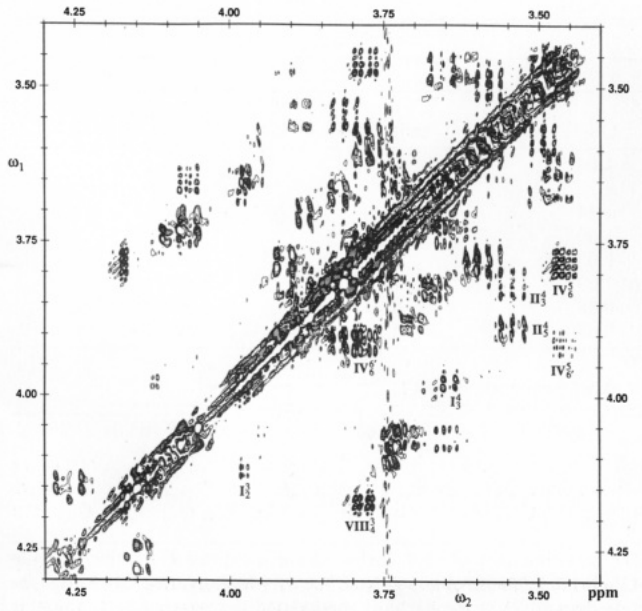

FIGURE 4: DQF-COSY spectrum (4.30–3.40 ppm) of the endo-OS-1 at 19.8 °C. The endo-OS-1 (the heptaose) was obtained from the dephosphorylated OS-1 after the endo enzyme treatment. Only some of the cross-peaks are labeled. The digital resolution of the spectrum is 0.78 Hz, and the cross-peaks are labeled as described in Figure 3.

of V (GalNAc) was not certain by the DQF-COSY and HOHAHA analysis, but it was assigned to be at 4.670 ppm from the intraresidual H1–H5 NOE. Similarly, the H-5 of both VII (Gal) and VIII (Gal) were identified to have the same chemical shifts to their H-3, which was evident by the larger NOE intensities for H-1 and H-3 of VII and VII than those of IV and V (Figure 6). Further, the interresidual NOE cross-speak between H-1 of VII (Gal) and H-4 of IV (GlcNAc) was found to overlap with the NOE cross-peaks due

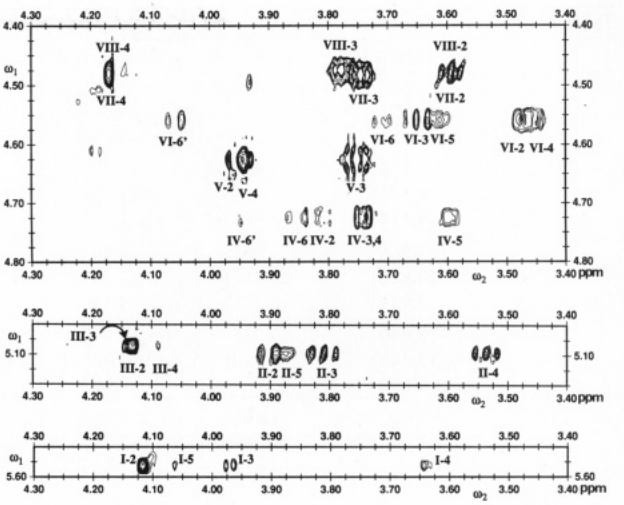

FIGURE 5: Parts of the HOHAHA spectrum (mixing time τ_m = 150 ms) of the dephosphorylated OS-1 at 19.8 °C. I, ManHep; II, GlcNAc; III, ManHep; IV, GlcNAc; V, GalNAc; VI, Glc; VII, Gal; VIII, Gal.

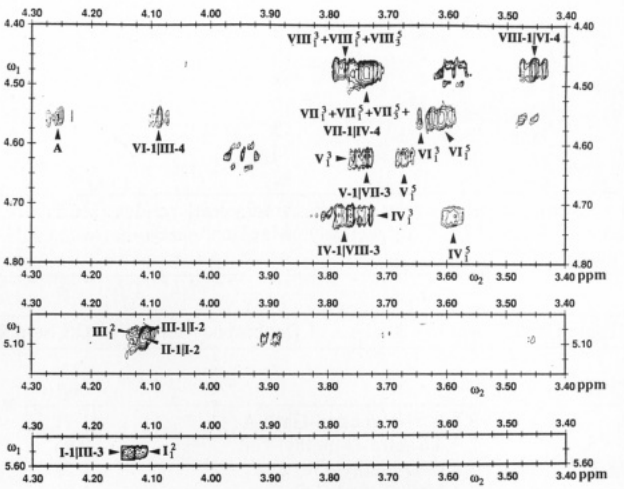

FIGURE 6: Parts of the pure-absorption 2D NOE spectrum (τ_m = 200 ms) of the dephosphorylated OS-1 at 19.8 °C. The interresidual NOE cross-peaks and some of the intraresidual ones are labeled. I, ManHep; II, GlcNAc; III, ManHep; IV, GlcNAc; V, GalNAc; VI, Glc; VII, Gal; VIII, Gal. (A) This interresidual NOE crosspeak is presumably due to H-1 of Glc (VI) and one of exocyclic protons of the ManHep (III). The 2D NOE spectrum (τ_m = 200 ms) of the endo-OS-1 was almost identical to that of the parent OS except for the absence of intra- and interresidual NOEs due to the GalNAcβ1→3Gal residue.

to the intraresidual 1,3-diaxially oriented protons (H1, H3, and H5) of VII, which was indicated by their larger NOE intensities than those of VIII. The interpretation of the above interresidual NOE will be discussed later. Under the experimental conditions used, no NOEs were observed between the cis 1,4-oriented protons (~3.8 Å) such as H1–H4 of the β-linked carbohydrates, IV–VIII, and H1–H3 or –H5 of II (α-GlcNAc). The strong intraresidual NOEs between H-1 and H-2 of both ManHep I and III also confirmed the manno configuration of both residues.

The structure of OS-1 was determined by comparative analysis of its interresidual NOE and methylation data with those of the endo enzyme treated OS-1. First, we determined the structure of the disaccharide, GalNAcβ→Gal, obtained after the endo enzyme treatment of the dephosphorylated OS-1. Methylation analysis of the disaccharide showed the presence of 2-acetamido-2-deoxy-*N*-methyl-3,4,6-tri-*O*-methylgalactosaminitol and 2,4,6-tri-*O*-methylgalactitol, from which we determined that the disaccharide is GalNAcβ1→-

Table I: ^{1}H NMR Chemical Shifts (ppm) and Coupling Constants (Hz) of Dephosphorylated F62 OS Components[a]

	ManHep I	GlcNAc II	ManHep III	GlcNAc IV	GalNAc V	Glc VI	Gal VII	Gal VIII
H-1	5.566	5.095	5.078	4.720	4.617	4.555	4.480	4.470
	(5.577)	(5.094)	(5.084)	(4.708)		(4.559)		(4.477)
	5.566	5.085	5.073	4.717		4.550	4.486	4.468
H-2	4.118	3.900	4.130	3.815	3.946	3.465	3.590	3.590
	(4.121)	(3.905)	(4.138)	(3.776)		(3.471)		(3.598)
	4.114	3.897	4.127	3.815		3.458	3.541	3.586
H-3	3.968	3.805	4.140	3.740	3.751	3.648	3.743	3.777
	(3.980)	(3.812)	(4.145)	(3.579)		(3.654)		(3.782)
	3.964	3.798	4.138	3.741		3.655	3.673	3.770
H-4	3.640	3.535	4.090	3.740	3.940	3.455	4.164	4.164
	(3.643)	(3.540)	(4.905)	(3.494)		(3.465)		(4.174)
	3.632	3.529	4.083	3.742		3.453	3.927	4.168
H-5	~4.06	3.875	3.725	3.595	3.670	3.609	~3.74	~3.77
	(4.065)	(3.886)	3.737	(3.545)		(3.622)		~3.78
	3.632	3.877	3.724	3.587		3.609	~3.67	~3.77
H-6				3.850		3.710		
				(3.779)		(3.716)		
				3.855		3.706		
H-6′				3.955		4.060		
						(4.060)		
				3.957		4.055		
$J_{1,2}$	3	4	3	9	8	9	8	8
$J_{2,3}$	4	10	3	11	10	10	10	10
$J_{3,4}$	4	8	4	8	3	8	4	4
$J_{4,5}$	7	10	8	10	4	9	3	3
$J_{5,6}$		3		5		7		
$J_{5,6'}$		6		3		2		
$J_{6,6'}$		12		13		13		

[a] Roman numerals refer to each carbohydrate residue (see Figure 2C). The top, middle, and bottom rows show the chemical shifts of the OS-1, endo-OS-1, and OS-2, respectively. ManHep, *manno*-heptose; GlcNAc, *N*-acetylglucosamine; GalNAc, *N*-acetylgalactosamine; Gal, galactose; Glc, glucose.

Table II: Methylation Analysis of Dephosphorylated F62 OS Samples

Part A[a]

	t_R	OS-1	endo-OS-1	OS-2
3,4,6-tri-*O*-methyl-GalNAc	1.21	1.04	–	–
2,3,4,6-tetra-*O*-methyl-Gal	0.93	–	–	1.09
3,6-di-*O*-methyl-GlcNAc	1.23	1.44	–	0.72
2,4,6-tri-*O*-methyl-Gal	1.00	1.00	1.00	1.00
2,3,6-tri-*O*-methyl-Glc	0.99	2.03	1.73	1.18
3,4,6-tri-*O*-methyl-GlcNAc	1.17	1.09	1.52	0.45
3,4,6,7-tetra-*O*-methyl-Hep	1.14	0.88	0.74	0.95
2,6,7-tri-*O*-methyl-Hep	1.18	0.68	0.67	0.78

Part B[b]

	m/z (% of base peak, *m/z* 43)				
tri-*O*-methyl-Hep	45 (18.0)	59 (12.3)	87 (5.2)	89 (7.2)	118 (65.0)
	378 (19.0)				
tetra-*O*-methyl-Hep	45 (29.8)	59 (22.9)	88 (29.0)	89 (25.6)	99 (17.6)
	100 (12.3)	101 (12.6)	113 (12.6)	130 (41.9)	173 (5.2)
	190 (17.4)	205 (24.7)			

[a] Relative retention times (t_R) are referenced to 2,4,6-tri-*O*-methyl-Gal. The mass intensity of each carbohydrate is expressed relative to 2,4,6-tri-*O*-methyl-Gal. (–) Not detected; OS-1, the dephosphorylated OS-1; endo-OS-1, the heptaose obtained from the dephosphorylated OS-1 after the endo enzyme treatment; OS-2, the dephosphorylated OS-2. [b] The alditol acetate derivatives of the partially methylated hexoses and hexosamine in the table gave identical fragmentation patterns to those of authentic samples. Major fragments obtained from the tri-*O*-methyl- and tetra-*O*-methylheptitol peracetates are shown in part B and below.

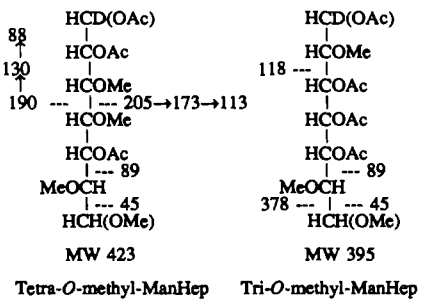

3Gal as suggested from the specificity of the enzyme (Kannagi et all, 1982). This disaccharide structure was also confirmed by the presence of the interresidual NOE between the H-1 of GalNAc (V) and H-3 of Gal (VII) of the dephosphorylated OS-1 (Figure 6).

Compared with the parent OS, the chemical shifts of endo-OS-1 are amost identical except a residue, IV (its anomeric proton at 4.720 ppm) (Table I and Figures 3 and 4). In particular, its H-4 was shielded upfield compared with that of OS-1 (3.494 vs 3.740 ppm), which suggested that the GalNAcβ1→3Gal(VII) is linked to the 4-position of this residue, IV. The presence of this linkage and the identity of IV being GlcNAc were confirmed by methylation and NOE data analysis. As shown in Table II, the 4-linked GlcNAc (3,6-di-*O*-methyl-GlcNAc) was present in the OS-1 but not in the endo-OS-1. Instead, the endo-OS-1 contained more terminal GlcNAc (3,4,6-tri-*O*-methyl-GlcNAc) than the parent OS, which indicated the new nonreducing end of the OS-1 after the endo enzyme treatment was GlcNAc. The data excluded the possibility of the disaccharide, GalNAcβ1→3Gal, being β1→4-linked to Glc instead of GlcNAc. The VII–IV structure was also supported by the NOE data (Figure 6) which indicated the overlap of the intraresidual NOEs of VIII (H-1, -3, and -5) and the interresidual NOE between H-1 of VII (Gal) and H-4 of IV. Since the chemical shifts of IV-3 and IV-4 are identical, the above interresidual NOE could be due to VII-1 and IV-3 or IV-4 or both. However, the involvement of H-3 was ruled out by the above methylation data. Also, under the experimental conditions, the interresidual NOE between VII-1 and IV-3 would not be expected with the Gal(VII)β1→4GlcNAc(IV) moiety. For example, the interresidual NOE due to VII-1 and VI-3 was not detected with the inner Gal(VII)β1→4Glc(VI) moiety, the structural determination of which will be described below. Thus, the trisaccharide GalNAcβ1→3Galβ1→4GlcNAc was confirmed to be present at the nonreducing terminus of the OS-1. Also, the presence of the terminal GlcNAc in the OS-1 showed that the OS has a branched structure which will be described later.

The above trisaccharide, GalNAc(V)β1→3Gal(VII)β1→-4GlcNAc(IV), was determined to be β1→3-linked to the following trisaccharide: Gal(VIII)β1→4Glc(VI)β1→-4ManHep(III). This structure was supported by the following data of the OS-1 that are also common to the endo-OS-1: (1) the interresidual NOE due to H-1 of GlcNAc (IV-1 at 4.720 ppm) and H-3 of Gal (VIII-3 at 3.777 ppm) (Figure 6); (2) the presence of the 3-linked Gal (2,4,6-tri-*O*-methyl-Glc) (Table II); (3) the interresidual NOE due to H-1 of Gal (VIII-1 at 4.470 ppm) and H-4 of Glc (VI-4 at 3.455 ppm); (4) the presence of the 4-linked Glc (2,3,6-tri-*O*-methyl-Glc); (5) the absence of the 4-linked GlcNAc in endo-OS-1, which confirmed the identity of VI being Glc; (6) the interresidual NOE due to H-1 of Glc (VI-1 at 4.555 ppm) and H-4 of ManHep (III-4 at 4.090 ppm) [the VI-1 also showed the interresidual NOE with a proton centered 4.250 ppm (Figure 6); this proton was not assigned but was suggested to be one of the exocyclic protons of ManHep (III)]; (7) the presence of the 3,4-linked heptose (2,6,7-tri-*O*-methyl-Hep), the identification of which will be described below.

A disaccharide, GlcNAc(II)α1→2ManHep(I), was found to be α-3-linked to the ManHep (III) of the hexaose GalNAcβ1→3Galβ1→4GlcNAcβ1→3Galβ1→4Glcβ1→-4ManHep(III). The branched structure (Figure 7) was confirmed by the presence of a terminal GlcNAc and 2,6,7-tri-*O*-methyl- and 3,4,6,7-tetra-*O*-methyl-Hep in the methylation analysis (Table II). We determined the identities of

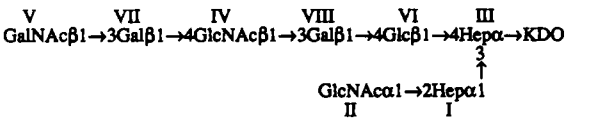

FIGURE 7: Proposed structure for the MAb 1-1-M defined OS component. The MAb 3F11 defined OS does not have a GalNAc residue at the nonreducing end, and the rest of the structure is identical to that of OS-1. GalNAc, *N*-acetylgalactosamine; Gal, galactose; GlcNAc, *N*-acetylglucosamine; Glc, glucose; Hep, heptose; KDO, 3-deoxy-2-ketooctulosonic acid.

the above heptoses from their mass fragmentation patterns. The structure of the tri-*O*-methyl-Hep was supported by the absence of the *m/z* 118 and the presence of the *m/z* 45, 89, 190, and 205. The 3,4-di-linked structure was determined by the presence of the *m/z* 89, 118, and 378 (splitting between C6 and C7).

Also, the above structure was supported by the following 2D NOE data: (1) the interresidual NOE cross-peak between the H-1 of ManHep (I-1 at 5.566 ppm) and H-3 of ManHep (III-3 at 4.130 ppm) (Figure 6); (2) the interresidual NOE due to H-2 of Hep (I-2 at 4.118 ppm) and H-1 of GlcNAc (II-1 at 5.095 ppm). The latter crosshpeak was partially overlapped with the one due to the H-1 of Manhep (III-1 at 5.078 ppm) and a proton centered at 4.118 ppm, and this proton was determined to be H-2 of ManHep (I-2). The detection of this interresidual NOE indicated that ManHep (III) is located above ManHep (I).

On the basis of the present data, we conclude the structure of the OS-1 to be as shown in Figure 7. ManHep (III) was determined to be linked to a reducing end carbohydrate, KDO, since ManHep (III) is the only carbohydrate remaining unlinked through its reducing end. Although the linkage between ManHep (III) and KDO was not determined in the present study, we found that the KDO at the reducing terminus does not exist as its pyranose or furanose form. In the DQF-COSY spectra of the intact or dephosphorylated OS samples, no cross-peaks were detected among the protons (presumably deoxy protons) that were located in the higher field. For example, the deoxy protons at 1.180, 1.325, 1.915, and 2.410 ppm in Figure 2C (the dephosphorylated OS-1) showed their cross-peaks with protons in the area of methyne and hydroxymethylene protons (data not shown). If the KDO at the reducing terminus is in equilibrium of the anomers of pyranose and furanose as found in a monomeric KDO (Cherniak et al., 1979), we would detect their H3a–H3e cross-peaks that contain large geminal couplings (McNicholas et al., 1986). The absence of the cross-peaks among the above deoxy protons also excludes the possibility of the KDO being a 2,8-anhydro derivative (McNicholas et al., 1987). The structure of the KDO is neither a pyran nor a furan derivative that has been reported (Charon & Szabó, 1973) since they do not have methyne protons that would resonate in a higher field. The KDO at the reducing terminus may exist as a 1,4-lactone structure (an enol form being dominant) (Charon & Szabó, 1973) or as a 4,8-anhydro form in which the $CH_2C(O)COOH$ is endocyclic. The formation of the 1,4-lactone from KDO under mild acidic conditions has been reported (Charon & Szabó, 1973), and the 4,8-anhydro derivative can also be expected from an O-4-substituted (e.g., phosphate) KDO as found in the case of sialic acid (*N*-acetylneuraminic acid) (Pozsgay et al., 1987).

The structure of OS-2 was determined to be the de-*N*-acetylgalactosaminilated OS-1. The 1D spectra of the β-*N*-acetylhexosaminidase-treated OS-1 and the OS-2 were almost identical. Also, DQF-COSY spectra of the endo enzyme treated OS-1 and the β-galactosidase-treated OS-2 (data not

shown) were identical. The structure of OS-2 was also supported by methylation analysis (Table II). From the present results, we conclude that the structure of the two OS components are identical except GalNAc which is present only in the OS-1.

Previously, we reported that the endo enzyme cleaved the MAb 1-1-M defined LOS component and its OS but not the MAb 3F11 defined LOS and its OS (Yamasaki et al., 1991). We were not able to explain this inactivity of the enzyme toward the MAb 3F11 defined LOS component because MAb 1-B-2 (Young et al., 1981), specific for the paragloboside (Galβ1→4GlcNAcβ1→3Galβ1→4Glcβ-ceramide), binds to the MAb 3F11 defined LOS component (Mandrell et al., 1988), and the paragloboside is cleaved by the endo enzyme (Fukuda, 1985). However, the present structural study resolved the above discrepancy. The endo enzyme is also known to cleave two internal β-galactosyl linkages of GalNAcβ1→3Galβ1→4GlcNAcβ1→3Galβ1→4Glcβ1→ceramide (Kannagi et al., 1982). Although the same pentaose structure is present in the MAb 1-1-M defined LOS component, the cleavage of the inner β-galactosyl linkage did not take place as expected from the results of the MAb 3F11 defined LOS component. These results suggest that this inactivity of the endo enzyme is due to steric hindrance caused by the presence of the branched diheptose structure (Figure 7).

We achieved the separation of the F62 OS components by ascending Bio-Gel P-4 chromatography after dephosphorylation by HF. We also tried other columns such as TSK-PW columns, reverse-phase columns, Mono-Q columns, and carbohydrate analysis columns. However, oligosaccharides carrying negative charges (KDO) at their reducing ends behaved completely differently in comparison with those whose nonreducing ends are negatively charged (sialylated), and two F62 OS components were not resolved by any of the above columns. We found that the base-line separation of gonococcal OS can be achieved by high-performance anion-exchange chromatography, and the results will be published elsewhere.

The present report is the only complete structural analysis of gonococcal OS, although there have been several reports on structural characterization of gonococcal OS (Perry et al., 1978; Connelly et al., 1983; Gibson et al., 1989). We determined the structures of the two OS components by chemical, enzymatic, and 2D NMR methods. The OS components, OS-1 and OS-2, obtained from the MAbs 1-1-M and 3F11 defined LOS components were found to be a nonaose and an octaose, respectively, and they both have a branched diheptose structure. The MAb 1-1-M defined OS component has a V^3-(β-*N*-acetylgalactosaminyl)neolactotetraose in which GalNAc is β1→3-linked to neolactotetraose at one of the nonreducing termini (Figure 7). This pentaose is identical to the OS structure of asialo-G_3 ganglioside, and the intact G_3 ganglioside has been isolated from human type O erythrocyte membrane (Watanabe & Hakomori, 1979). The above pentaose is β-linked to a branched diheptose–KDO core, and GlcNAc is α-linked to one of the heptoses. The MAb 3F11 defined OS does not have a terminal GalNAc, and a neolactotetraose is exposed at its nonreducing terminus. The structural difference of the two OS components is GalNAc which is present only in the OS-1.

The LOS F62 is from a serum-sensitive strain and consists of two components that are defined by MAbs 1-1-M and 3F11 (Yamasaki et al., 1988, 1991). The above two MAbs recognize many strains of gonococci (Mandrell et al., 1986; Schneider et al., 1984). Previously, we showed that the specificities of MAbs 1-1-M and 3F11 are directed toward the nonreducing termini of the LOS components (Yamasaki et al., 1991). The present structural data indicate that the above IgM-defined LOS epitopes are in the longer oligosaccharide moiety of each LOS component. However, the epitopes are not simply the linear oligosaccharide structure at the nonreducing termini; their expression is also conformational (Yamasaki et al., 1988).

The antigenic similarity of the gonococcal LOS to human glycosphingolipids has been shown by immunochemical analysis of LOS and glycosphingolipids (Mandrell et al., 1988; Stromberg et al., 1988). However, this antigenic similarity was not defined in terms of the LOS structure. Our structural study fills this gap and will provide the basis for us to understand the antigenicity and immunogenicity of gonococci. We are conducting the structural analysis of gonococcal LOS of a serum-resistant strain and will be able to define the structural basis for the serum sensitivity of the gonococcus.

ACKNOWLEDGMENTS

We thank Kevin Quinn for carrying out the Dionex and methylation analysis. We also thank Dr. Deborah Kerwood for conducting the DQF-COSY experiment of the β-galactosidase-treated OS-2.

REFERENCES

Bax, A., & Davis, D. G. (1985) *J. Magn. Reson. 65*, 355–360.
Charon, D., & Szabó, L. (1973) *J. Chem. Soc., Perkin. Trans. 1*, 1175–1179.
Cherniak, R., Jones, R. G., & Gupta, D. S. (1979) *Carbohydr. Res. 75*, 39–49.
Ciucanu, I., & Kerek, F. (1984) *Carbohydr. Res. 131*, 209–217.
Connelly, M. C., & Allen, P. Z. (1983) *Carbohydr. Res. 120*, 171–186.
Fukuda, M. (1985) *Biochemistry 24*, 2154–2163.
Gibson, B. W., Webb, J. W., Yamasaki, R., Fisher, S. J., Burlingame, A. L., Mandrell, R. E., Schneider, H., & Griffiss, J. M. (1989) *Proc. Natl. Acad. Sci. U.S.A. 86*, 17–21.
Gregg, C. R., Melly, M. A., Hellerqvist, C. G., Coniglio, J. G., & McGee, Z. A. (1981) *J. Infect. Dis. 143*, 432–439.
Griffiss, J. M., O'Brien, J. P., Yamasaki, R., Williams, G. D., Rice, P. A., & Schneider, H. (1987) *Infect. Immun. 55*, 1792–1800.
Hardy, M., Townsend, R. R., & Lee, Y. C. (1988) *Anal. Biochem. 170*, 54–62.
Kannagi, R., Fukuda, M. N., & Hakomori, S. (1982) *J. Biol. Chem. 257*, 4438–4442.
Levery, A. S. B., & Hakomori, S. (1987) *Methods Enzymol. 138*, 13–25.
Mandrell, R. E., Schneider, H., Apicella, M., Zollinger, W., Rice, P. A., & Griffiss, J. M. (1986) *Infect. Immun. 54*, 63–69.
Mandrell, R. E., Griffiss, J. M., & Macher, B. J. (1988) *J. Exp. Med. 168*, 107–126.
McNicholas, P. A., Batley, M., & Redmond, J. W. (1986) *Carbohydr. Res. 146*, 219–231.
McNicholas, P. A., Batley, M., & Redmond, J. W. (1987) *Carbohydr. Res. 165*, 17–22.
Neuhaus, D., Wagner, G., Vasak, M., Kagi, J. H. R., & Wüthrich, K. (1985) *Eur. J. Biochem. 151*, 257–273.
Osborn, M. J. (1983) *Proc. Natl. Acad. Sci. U.S.A. 50*, 499–506.
Paruchuri, D. K., Seifert, H. S., Ajikoa, R. S., Karlsson, K. A., & So, M. (1990) *Proc. Natl. Acad. Sci. U.S.A. 87*, 333–337.

Perry, M. B., Daoust, V., Johnson, K. G., Diena, B. B., & Ashton, F. E. (1978) in *Immunobiology of Neisseria gonorrhoeae* (Brooks, F. B., Gotschlich, E. G., Holmes, K. K., Sawyer, W. D., & Young, F. E., Eds) pp 101–107, American Society of Microbiology, Washington, DC.

Pozsgay, V., Jennings, H., & Kasper, D. L., (1987) *Eur. J. Biochem. 162*, 445–450.

Rance, M., Sorensen, O. W., Bodenhausen, G., Wagner, G., Ernst, R. R., & Wüthrich, K. (1983) *Biochem. Biophys. Res. Commun. 117*, 479–485.

Redfield, A. G., & Kunz, S. D., (1975) *J. Magn. Reson. 19*, 250–254.

Schneider, H., Griffiss, J. M., Williams, G. D., & Pier, G. B. (1982) *J. Gen. Microbiol. 128*, 13–22.

Schneider, H., Hale, L., Zollinger, W., Seid, R. C., Jr., Hammack, C. A., & Griffiss, J. M. (1984) *Infect. Immun. 45*, 544–549.

Schoolnik, G. K., Buchanan, T. M., & Holmes, K. K. (1976) *J. Clin. Invest. 58*, 1163–1173.

States, D. J., Haberkorn, R. A., & Ruben, D. J. (1982) *J. Magn. Reson. 48*, 286–292.

Stromberg, N., Deal, C., Nyberg, G., Normark, S., So, M., & Karlsson, K. A. (1988) *Proc. Natl. Acad. Sci. U.S.A. 85*, 4902–4906.

Stults, C. L. M., Sweeley, C. C., & Macher, B. (1989) *Methods Enzymol. 179*, 167–214.

Watanabe, K., & Hakomori, S. (1979) *Biochemistry 18*, 5502–5504.

Yamasaki, R. (1988) *Biochem. Biophys. Res. Commun. 154*, 159–164.

Yamasaki, R., & Bacon, B. E. (1991) *Biochemistry 30*, 851–857.

Yamasaki, R., Schneider, H., Griffiss, J. M., & Mandrell, R. (1988) *Mol. Immunol. 25*, 799–809.

Yamasaki, R., Nasholds, W., Schneider, H., & Apicella, M. A. (1991) *Mol. Immunol.* (in press).

Young, W. W., Jr., Portoukalian, J., & Hakomori, S. (1981) *J. Biol. Chem. 256*, 10967–10972.